1-1-2008

Investigation of p-GaAsSb as a THz Emitter

Stuart Hargreaves
University of Wollongong, sh64@uow.edu.au

L. J. Bignell
University of Wollongong

Roger A. Lewis
University of Wollongong, roger@uow.edu.au

D Schoenherr
Technische Universitat Darmstadt

M Saglam
Technische Universitat Darmstadt

See next page for additional authors

Journal of The Electrochemical Society, **155** (10) H734-H737 (2008)
0013-4651/2008/155(10)/H734/4/$23.00 © The Electrochemical Society

Investigation of p-GaAsSb as a THz Emitter

S. Hargreaves,[a] L. J. Bignell,[a] R. A. Lewis,[a,z] D. Schoenherr,[b] M. Sağlam,[b] and H. L. Hartnagel[b,*]

[a]*Institute for Superconducting and Electronic Materials, University of Wollongong, Wollongong, New South Wales 2522, Australia*
[b]*Institut fuer Hochfrequenztechnik, Technische Universitaet Darmstadt, 64283 Darmstadt, Germany*

Our purpose was to determine if GaAsSb might be made to emit THz-frequency electromagnetic radiation. Our result is that, with a suitable electric field imposed and under illumination by ultrashort pulses of near-infrared radiation, GaAsSb indeed emits THz radiation. To the best of our knowledge this is the first report of high-temperature-grown GaAsSb acting as a THz source. THz emission has been observed both by incoherent (pneumatic Golay cell) and by coherent (time-domain spectroscopy using electro-optic detection) experimental configurations. Both simple Ag paint and photolithographically formed Au on Ti antenna structures have been found to produce THz radiation. We compare our results with those from the better-known THz emitter, GaAs. In the case of GaAs, THz radiation is emitted even in the absence of applied bias. This is not the case for GaAsSb. We conclude that the photoconductive mechanism dominates in the emission of THz radiation from epitaxial single-crystal GaAsSb. A further proposal is made that such materials can be used with nanostructured surfaces for special THz-emission characteristics.
 [DOI: 10.1149/1.2961065]

Manuscript received June 2, 2008. Published August 5, 2008; publisher error corrected September 5, 2008.

The field of terahertz (THz = 10^{12} Hz) science and technology is rapidly developing. THz spectroscopy is being used to characterize many materials, including packaging, explosives, and drugs. A recent application has been to characterize single-wall nanotube thin-film electrodes.[1] In another approach, using a separate pump beam to excite charge carriers in a material shortly before the THz analysis is carried out, information about ultrafast carrier dynamics may be obtained. A recent example of such time-resolved THz measurement deals with poly(3-hexylthiophene) and methanofullerene blended films.[2]

In spite of much study over recent years, the development of THz emitters is far from complete. The materials most commonly employed as THz emitters are semiconductors under a higher-frequency laser excitation. Semiconductors such as ZnTe exhibit strong optical nonlinearity and so may produce THz radiation by optical rectification. Other semiconductors, such as InAs, emit THz radiation through a surface-field (SF) effect. Furnished with suitable electrode or antenna structures, others again generate THz radiation by the photoconductive (PC) mechanism. Low-temperature (LT)-grown GaAs is the best known of the PC emitters. Recent reports on semiconductor THz emitters include the enhancement of emission by conjugate polymer[3-5] and stimulated THz emission from acceptor-doped strained p-Ge and SiGe/Si quantum-well structures.[6,7] In this paper we investigate acceptor-doped GaAsSb as a candidate THz emitter.

GaAsSb has been long known, and is still employed, as a suitable material for the realization of heterostructures and other quantum devices.[8,9] Technical developments continue to occur in such areas as GaAsSb etching[10] and the production of ohmic contacts on p-GaAsSb.[11] Regarding applications as a THz emitter, both LT-grown $GaAs_{0.6}Sb_{0.4}$[12] and LT-grown $GaAs_{0.81}Sb_{0.19}$[13] have been demonstrated to produce THz under suitable laser excitation. Alloying with Sb decreases the bandgap relative to GaAs and so permits the use of longer-wavelength laser excitation than conventionally employed with LT-GaAs THz emitters. We have recently investigated the THz emission from Be-doped GaAs.[14,15] In the present work, we extend the investigation to Be-doped GaAsSb.

Experimental

GaAsSb layers were grown lattice-matched on semi-insulating InP substrates by molecular-beam epitaxy. Ex situ X-ray diffraction determined the Sb fraction to be 0.487, exactly the value estimated from the GaAs and GaSb lattice constants to lattice match InP. By linear interpolation from the GaAs and GaSb values, the bandgap is estimated to be 1.06 eV. The layers were nominally 1 μm thick. In the sense that quantum confinement effects are not involved, they may be referred to as "bulk." A nominally undoped sample was grown, as well as samples doped with the acceptor Be at concentrations of nominally 2×10^{17}, 1×10^{18}, and 1×10^{19} cm^{-3}, respectively. After growth, the samples were annealed at 400°C in an H_2 atmosphere for 10 min. Details of the layer thicknesses, as well as the Hall mobilities and carrier concentrations at 77 and 300 K, are set out in Table I.

The layers were characterized by optical-reflectance measurements over the range 3–18 THz. These data were collected on a Bomem DA3 rapid-scan spectrometer, which was evacuated to reduce absorption by atmospheric water vapor. The principal optical elements were a silicon carbide (globar) source, a mylar beam splitter, and a deuterated triglycerine sulfide detector. Samples were examined in near-normal incidence geometry, and polished brass was used as a reflectance reference. The spectral resolution was 0.012 THz.

To permit photoconductivity measurements, electrical connections were made to the samples. Two types of contacts were used. Silver paint electrodes of approximately 0.1 mm gap were found to be simple to fabricate and reasonably reproducible.[16] Gold-on-titanium bow-tie antennas were fabricated by standard UV photolithography followed by lift-off.[17] The Ti served as an adhesion layer and was 10 nm thick; the Au top layer was 100 nm thick. Electrical characterization utilized a Keithley 2400 SourceMeter.

To generate THz radiation using the samples as targets, the optical excitation was provided by a 12-femtosecond mode-locked Ti:sapphire laser of center frequency 790 nm and repetition rate 75 MHz. The emitted THz radiation was detected either using a pneumatic Golay cell (incoherent detection) or in a conventional time-domain spectroscopy arrangement using electro-optic (coherent) detection.

Results and Discussion

The reflectance data for all four samples is shown in overview in Fig. 1. This figure also includes our data for reflectance from bulk InP, the substrate material. The resonance associated with the GaAsSb layer is clear for all samples, peaking in reflectance at about 7.5 THz. The prominent feature spanning approximately 9–10.5 THz is associated with the substrate, as may be seen from comparison with the InP spectrum. The notch in the reststrahlen of the InP substrate deepens with increasing GaAsSb-layer carrier concentration. The small "bump" seen in some spectra at approximately 7 THz corresponds closely to the phonon energy of GaSb, suggesting that the alloy may exhibit a mixed-mode behavior. A thorough

* Electrochemical Society Active Member.
z E-mail: roger@uow.edu.au

Table I. The GaAsSb samples employed in this study. The mobility, μ, and charge-carrier concentration, n_v, as determined by Hall measurements, are given at 300 and 77 K for the three intentionally doped samples.

	A	B	C	D
GaAsSb layer thickness (nm)	800	900	900	900
Hall measurements at 300 K				
μ (cm^2/V s)		7564	4593	2401
n_v (cm^{-3})	Undoped	2.04×10^{17}	1.02×10^{18}	9.24×10^{18}
Hall measurements at 77 K				
μ (cm^2/V s)		9288	5335	2643
n_v (cm^{-3})	Undoped	1.94×10^{17}	1.02×10^{18}	9.59×10^{18}

study of this material has been conducted by Lucovsky and Chen[18] and shows the mixed-mode behavior more conclusively. To avoid unnecessary complication in fitting the data, this GaSb-like feature was not included as another oscillator in the model, but rather $GaAs_{1-x}Sb_x$ with alloying parameter $x = 0.48$ was used. The data was fitted with a matrix model of optical reflectance, as described previously.[19]

Figure 2a gives the data for the nominally undoped sample, together with the model fit. Surprisingly, as this is the simplest sample, it gave the poorest of the fits to the data out of the series. There appears to be a mismatch of the layer reflection. This is most likely caused by the GaSb-like resonance, which is the strongest in this sample. (The addition of a GaSb-like oscillator in the layer provided a worse fit.) Although the results for the layer were poor, the results for the substrate were as expected. While the layer is nominally undoped, the observation of a notch in the InP reststrahlen peak is an unmistakable indicator of the presence of charge carriers. The layer thickness from the fit was approximately twice the nominal value. This was a trend that was observed among all the samples. Fitting parameters are given in detail in Table II.

Figure 2b gives the data for the least-heavily intentionally doped sample along with the model fit. The fitting parameters were all generally in good agreement with the interpolated values of the phonon energy as well as the dielectric constants of the alloy. The plasma frequency was predicted using the nominal value of the carrier concentration and a linearly interpolated value of the hole effective mass.[20] The plasma frequency found from the model fit is in good agreement with the Hall value (Tables I and II).

The data with fits for the two remaining samples are given in Fig. 2c and d. The model generally accounts for the experimental data well. In both cases the plasma frequency obtained by the fitting was somewhat less than the value calculated on the basis of the Hall hole concentration and the interpolated value of the effective mass. This is not entirely unexpected, as the Hall data is essentially a dc measurement, whereas the reflectance characterization is at optical frequencies. The fitting parameters are again given in Table II.

Before attempting to detect THz emission, photoconductivity measurements were made on the samples by measuring the electrical characteristics under different levels of laser illumination. The results of such an experiment are shown in Fig. 3. Here the current flowing between the Ag paint electrodes is given as a function of applied bias (in the range 0–52 V) for the nominally undoped sample under illumination of (*i*) 90 and (*ii*) 240 mW of pump laser radiation. It may be observed that the increase in excitation power induces an increase of current at a given bias, i.e., photoconductivity, but that the effect is rather small. It is much smaller than effects we have observed previously in GaAs.[15]

The doped samples were also tested for photoconductivity, but none of them gave a measurable response. This was because they were all highly conductive to begin with, at least an order of magnitude more conductive than the nominally undoped sample. This meant that only a significantly lower bias could be applied before Joule heating led to thermal runaway. As well, it meant that the application of the pump radiation had little room to increase the sample conductivity.

The THz emitted was first sought in a straight-through transmission geometry using a Golay cell as the detector. In the case of incoherent detection, such as with a Golay cell, there is the possibility that a bolometric signal is received merely as a result of the sample being heated by the pump beam, as distinct from a coherent THz pulse being generated by the pump pulse. This possibility of

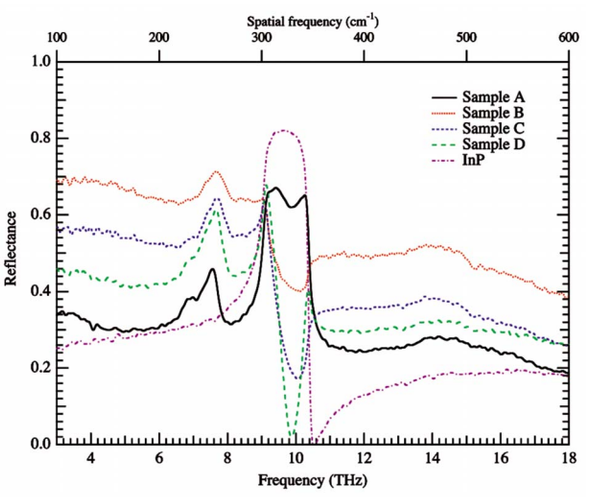

Figure 1. (Color online) Overview of reflectance spectra of GaAsSb samples of different doping levels with Be acceptor. The spectrum for InP (substrate material) is shown for comparison.

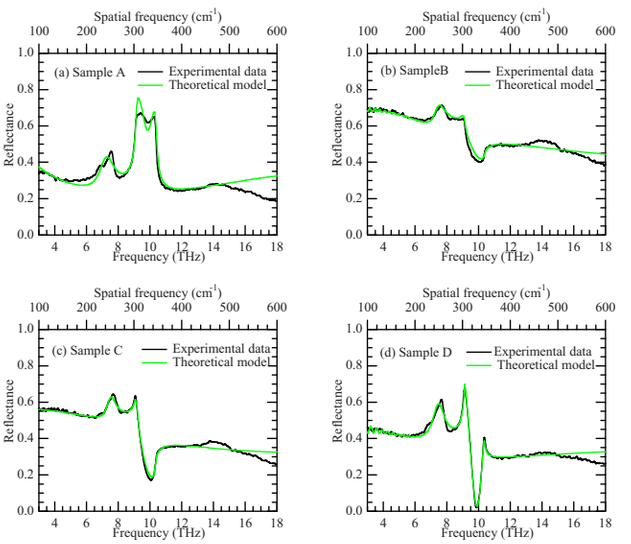

Figure 2. (Color online) Reflectance spectra of GaAsSb samples of different doping levels with the Be acceptor together with the theoretical model;[19] (a) sample A, (b) sample B, (c) sample C, and (d) sample D.

Table II. Fitting parameters of a two-layer matrix model to the optical reflectance data of the GaAsSb samples employed in this study. For further details of the model and the parameters, see Ref. 19.

	A	B	C	D
GaAsSb layer				
ε (0)	11.6	14.6	14.4	14.1
ε (∞)	10.6	13.7	13.4	12.7
ω_T (THz)	7.20	7.36	7.48	7.43
Γ (THz)	0.75	0.57	0.48	0.51
Plasma				
ω_p (THz)	3.66	7.62	10.29	6.33
Γ (THz)	~0	5.16	11.82	7.77
Thickness				
t (μm)	1.54	1.60	1.38	1.39
InP substrate				
ε (0)	12.8	12.3	11.8	12.8
ε (∞)	9.9	9.4	9.2	10.0
ω_T (THz)	9.15	9.08	9.12	9.13
Γ (THz)	0.10	0.08	0.05	0.06

spurious signal was ruled out by making measurements first with no laser illumination and secondly with maximum laser illumination but under continuous-wave conditions (as opposed to pulsed or mode-locked operation). In both cases, no signal was detected above the noise floor, regardless of the applied bias. We are thus confident that the observed signal is due to coherent THz emission. Some representative data are shown in Fig. 4. The amount of THz radiation emitted increases with applied bias, as would be expected. The rate of increase at first increases with bias, as is the case for GaAs, where a quadratic dependence of radiated THz power on applied bias is observed.[15] Beyond about 25 V applied bias, however, the rate of increase declines, tending toward a linear dependence of the THz power on bias. The reason behind this saturation effect is not known precisely but may be related to an increase in sample resistance or a decrease in mobility due to heating. The THz power also increases directly with optical excitation power, as might be expected (Fig. 4) and as is the case for GaAs.[15]

The THz emission was next investigated using time-domain spectroscopy. For both the Ag paint and the Au antenna structure, representative time-domain spectra are shown in Fig. 5. The magnitudes of the detected THz electric fields are comparable in the two data sets shown, but the Ag paint data is for a higher applied bias

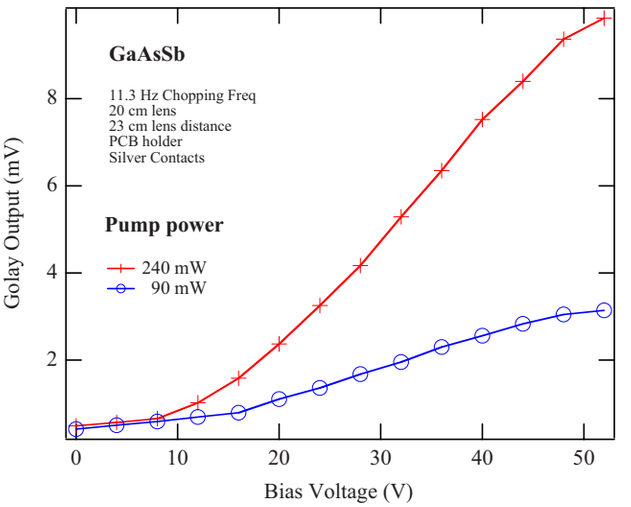

Figure 4. (Color online) THz signal from GaAsSb sample A as a function of applied bias and optical excitation power.

(12 V) than the Au antenna data (5 V). In general, the Au antennas produced a much stronger THz signal than the Ag-paint electrodes for a given applied bias. With the available carrier density in the semiconductor, evaporated metals (Ti/Au) give a better charge-carrier transfer behavior than painted metals, where the native oxide of the semiconductor surface is not broken down, and so charge transfer is impeded. It is likely that such phenomena are responsible for the observed behavior regarding the two types of metal contacts.

Figure 6 gives the frequency-domain power spectra resulting from the Fourier transform of the time-domain spectra of Fig. 5. It may be observed that the bandwidths of the two types of electrode structures are similar.

Finally, all four samples were extensively tested as SF emitters in a similar configuration as that used for the well-known SF emitter p-InAs.[21] The experimental method was to first use a p-InAs emitter to give a THz spectrum, then immediately replace it with a GaAsSb candidate emitter (no signal above the noise was observed), then finally swap the p-InAs material back in (again a strong THz signal was observed). Using this approach, we are confident that GaAsSb gives, at most, very little THz signal as a SF emitter. This is in contrast to GaAs, where we have observed a strong SF emission.

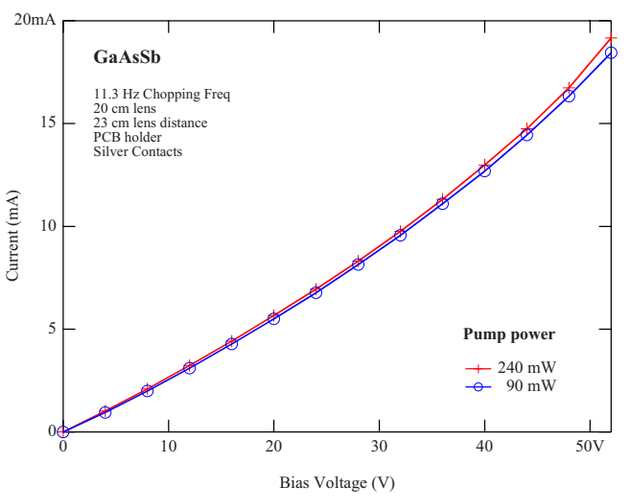

Figure 3. (Color online) PC response of GaAsSb sample A under pulsed near-infrared excitation.

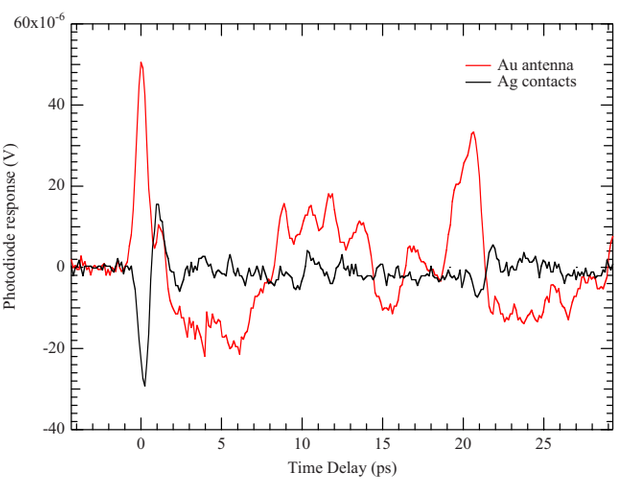

Figure 5. (Color online) Time-domain spectra of GaAsSb sample A for Ag and Au contacts.

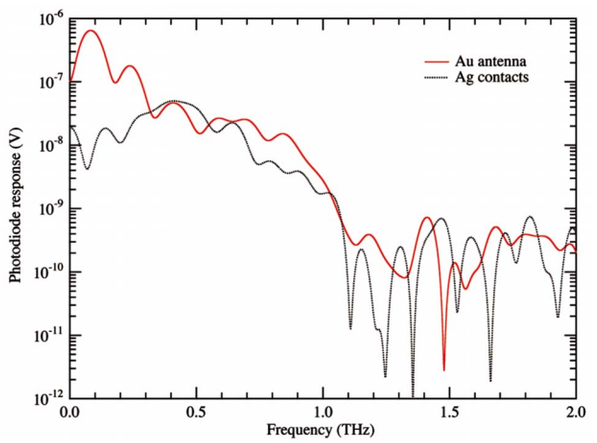

Figure 6. (Color online) Frequency-domain spectra of GaAsSb sample A for Ag and Au contacts.

Conclusion

The emission of THz radiation has been demonstrated in undoped, high-temperature-grown GaAsSb to take place by a PC mechanism. This material can therefore also be considered as a candidate for THz emission along with previously identified materials. High-temperature epitaxial growth means that the semiconductor is perfectly crystalline, in contrast to LT-grown materials, which are likely to be less stable and with an expected limited device life. Additionally, it is easier to produce nanometric structures on single-crystal material, which might be an interesting approach for further THz emission optimization.

Acknowledgments

The Australian Research Council supported this work. The cooperation was funded by the German DLR in the Federal Ministry of BMBF under AUS 05/003. This support is gratefully acknowledged.

References

1. J. Blackburn, T. Barnes, M. Beard, C. Engtrakul, T. McDonald, B. To, T. Coutts, and M. Heben, Abstract 1018, The Electrochemical Society Meeting Abstracts, Vol. 2008-1, Phoenix, AZ, May 18–22, 2008.
2. X. Ai, M. Beard, K. Knutsen, S. Shaheen, G. Rumbles, and R. Ellingson, Abstract 607, The Electrochemical Society Meeting Abstracts, Vol. 2006-1, Denver, CO, May 7–12, 2006.
3. J.-S. Hwang, H.-C. Lin, Y.-C. Huang, and K.-I. Lin, Abstract 1259, The Electrochemical Society Meeting Abstracts, Vol. 2007-2, Washington, DC, Oct 7–12, 2007.
4. J.-S. Hwang, H.-C. Lin, Y.-C. Huang, K.-I. Lin, J.-W. Chang, and T.-F. Guo, *ECS Trans.*, **11**(5), 59 (2007).
5. J. S. Hwang, H. C. Lin, Y. C. Huang, K. I. Lin, J. W. Chang, and T. F. Guo, *Electrochem. Solid-State Lett.*, **11**, H63 (2008).
6. M. S. Kagan, I. Altukhov, V. Sinis, E. Chirkova, S. Paprotskiy, I. Yassievich, M. Odnoblyudov, A. Prokofiev, and J. Kolodzey, Abstract 1476, The Electrochemical Society Meeting Abstracts, Vol. 2006-2, Cancun, Mexico, Oct 29–Nov 3, 2006.
7. M. S. Kagan, I. Altukhov, V. Sinis, E. Chirkova, S. Paprotskiy, I. Yassievich, M. Odnoblyudov, A. Prokofiev, and J. Kolodzey, *ECS Trans.*, **3**(7), 745 (2006).
8. G. A. Antypas and R. L. Moon, *J. Electrochem. Soc.*, **121**, 416 (1974).
9. T. Kuech, M. Rathi, A. A. Khandekar, D. Xu, J. Y. T. Huang, J. H. Park, L. Mawst, X. Song, and S. Babcock, Abstract 1258, The Electrochemical Society Meeting Abstracts, Vol. 2007-2, Washington, DC, Oct 7–12, 2007.
10. M. Lijadi, C. David, and J.-L. Pelouard, *Electrochem. Solid-State Lett.*, **8**, C189 (2005).
11. J. H. Jang, H. K. Cho, J. W. Bae, I. Adesida, and N. Pan, *J. Electrochem. Soc.*, **154**, H389 (2007).
12. J. Sigmund, C. Sydlo, H. L. Hartnagel, N. Benker, H. Fuess, F. Rutz, T. Kleine-Ostmann, and M. Koch, *Appl. Phys. Lett.*, **87**, 252103 (2005).
13. U. Willer, R. Wilk, W. Schippers, S. Böttger, D. Nodop, T. Schossig, W. Schade, M. Mikulics, M. Koch, M. Walther, et al., *Appl. Phys. B*, **87**, 13 (2007).
14. S. Hargreaves and R. A. Lewis, in *Joint 32nd International Conference on Infrared and Millimeter Waves and the 15th International Conference on Terahertz Electronics*, IEEE, p. 202 (2007).
15. S. Hargreaves, R. A. Lewis, and M. Henini, *Proc. SPIE*, **6798**, 67980Y (2007).
16. G. Zhao, R. N. Schouten, N. v. d. Valk, W. T. Wenckebach, and P. C. M. Planken, *Phys. Med. Biol.*, **47**, 3699 (2002).
17. C. Sydlo, R. Mendis, J. Sigmund, M. Feiginov, H. L. Hartnagel, and P. Meissner, *International Conference on Wireless Communications and Applied Computational Electromagnetics*, IEEE/ACES, p. 873 (2005).
18. G. Lucovsky and M. F. Chen, *Solid State Commun.*, **8**, 1397 (1970).
19. L. J. Bignell and R. A. Lewis, *J. Mater. Sci.: Mater. Electron.*, In press. [DOI: 10.1007/s10854-008-9608-2]
20. M. Levinshtein, S. Rumyantsev, and M. Shur, *Handbook Series on Semiconductor Parameters; Vol. 1—Si, Ge, C (Diamond), GaAs, GaP, InAs, and InSb*, World Scientific, Singapore (1999).
21. R. A. Lewis, M. L. Smith, R. Mendis, and R. E. M. Vickers, *Physica B*, **376–377**, 618 (2006).